III–V Compound Semiconductor Quantum Dots for Nanoeletronics

S. B. Krupanidhi

Abstract | Quantum dots have attracted considerable interest because their atom-like properties make them a good venue for studying physics of confined carriers and the ability to lead to novel device applications in fields such as quantum cryptography, quantum computing, optics and optoelectronics. Zero-dimensional semiconductor structures, or quantum dots (QDs), have attracted considerable interest for their atomic-like optical properties. In order to avoid non-radiative recombination defects caused by nano-fabrication processes, tremendous efforts have been focused on a one-step Stranski- Krastanow growth of self-assembled quantum dots, such as In(Ga)As/GaAs, InP/GaInP and GeSi/Si. In contrast, strain-induced quantum dots formed by locally straining a near surface quantum well with self-assembled islands can be modeled accurately. QW width is usually much smaller than the diameter of the stress or, the inhomogeneous broadening of each dot state is dominated by the QW interface fluctuation and is less influenced by the dot size variation. Various efforts are evident in the development of quantum dots of optically active materials such as compound semiconductors. Present review deals with some of the latest developments in the growth of quantum dots and their applications in opto-electronic devices.

Introduction

Quantum dots are often referred to as artificial atoms. A quantum dot is a very small chunk of semiconductor material with quantum-like properties.[1,2] Generally speaking quantum dots have a nexus with nanoparticles and nanocrystals. Nanoparticles can be just about anything whose dimensions are on the nanometer scale, while nanocrystals are usually nanometer-sized inorganic solids such as metals, insulators or semiconductors. 'Quantum dot' is a term usually applied to semiconductor nanocrystals in a size limit whose volume is smaller than the volume defined by the Bohr radius of that particular semiconductor. At these scales, there are effects that the bulk form of the same material does not possess. This phenomenon is called quantum confinement.

The electrons in quantum dots have a range of energies. The concepts of energy levels, bandgap, conduction band and valence band still apply. However, there is a major difference. Excitons have an average physical separation between the electron and hole, referred to as the "Exciton Bohr Radius" (D_B). This physical distance is different for each material. In bulk, the dimensions of the semiconductor crystal are much larger than the Exciton Bohr Radius, allowing the exciton to extend to its natural limit. However, if the size of a semiconductor crystal becomes small enough that it approaches the size of the material's Exciton Bohr Radius, then the electron energy levels can no longer be treated as continuous - they must be treated as discrete, meaning that there is a small and finite separation between energy levels.

Materials Research Centre, Indian Institute of Science Bangalore 560012

Figure 1: AFM micrograph of InAs grown.

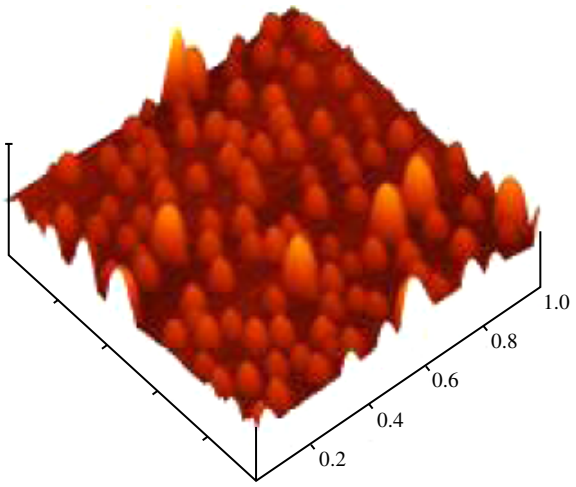

Quantum dots: Quantum dots are artificial atoms and are a very small chunk of semiconductor material with quantum-like properties.

This situation of discrete energy levels is called quantum confinement, and under these conditions, the semiconductor material ceases to resemble bulk. This is an inherently quantum phenomenon - hence the names, "quantum well", "quantum wire", and "quantum dot", which describe confinement in 1, 2 and 3 dimensions, respectively. 'D_B' is often used as a yard-stick to judge the extent of confinement in a low-dimensional structure. The confinement regimes describe a size range in semiconductor quantum dots that compare the Bohr radius to the diameter of the nanocrystal (D):

1. Strongly-confined regime: $D < 2D_B$
2. Intermediate confinement regime: $D \sim 2D_B$
3. Weakly-confined regime: $D > 2D_B$

It is in the **strongly-confined regime** that the optical properties of these quantum dots are most affected.

Epitaxy, in general

Quantum dots of compound semiconductors are generally grown through epitaxy approaches, using either MOCVD (metalorganic chemical vapor deposition) or MBE (Molecular Beam Epitaxy) techniques[3]. Epitaxy, in common with all forms of crystal growth, is in fact a well-controlled phase transition which leads to a single crystalline solid. Thus, the thermodynamics of phase transitions is the first basic tool we use to understand epitaxy. However, epitaxy is a dynamic and not an equilibrium process; and hence the need for a second tool, kinetics, both of mass transport and of surface processes. In epitaxy one distinguishes between homo-epitaxy, i.e. the growth of layers of the same material as the substrate (ignoring different doping) and hetero-epitaxy in which the single crystal layer material differs from the substrate. However, also in hetero-epitaxy it must be ensured that the lattice constant of both materials is roughly the same, as otherwise a single crystal film is not achieved due to high intrinsic stress[4].

Typically, the growth process consists of many sequential steps as illustrated in figure 1 for the growth of GaAs with Ga (A) and As(B) as the reactants. Thermodynamics drives the process A(b) + B(cr). The reactant A must diffuse from the bulk, A(b), to the growing surface, A(g). It then adsorbs onto the surface at a vacant site, to become A*. At this point, it can either desorb or react on the surface with other surface species (or simply decompose) to form B*. B* must diffuse along the surface to a low-energy site such as at the edge of a monatomic step where more than one bond can be formed, B_s*. B_s* then diffuses along the step to a kink where an additional bond can be formed and is incorporated into a 'half crystal' site in the lattice, B(cr). The incorporation reaction often releases one or more product molecules designated C*, which then desorbs and eventually diffuse into the bulk gas phase. Any one of these kinetic steps may be the slowest, and hence limit the overall reaction rate. A pictorial representation is presented in figure 2. to show the atomic arrangement during variety of processes those are prevalent during epitaxy.

Physics of Quantum Dots

The main challenges are to understand the way the one-electron levels of the dot reflect quantum size, quantum shape, interfacial strain, and surface effects, and the nature of "many-particle" interactions such as electron-hole exchange (underlying the "red shift"), electron-hole Coulomb effects (underlying excitonic transitions), and electron-electron Coulomb effects (underlying Coulomb-blockade effects)[5]. Interestingly, while the electronic structure theory of periodic solids has been characterized since its inception by a diversity of approaches the theory of quantum nanostructures has been dominated mainly by a single approach referred to as the "Standard Model": the effective-mass approximation (EMA) and its extension to the "k-p method" (where **k** is the wave vector and **p** is the momentum). The essential idea is sweeping in its simplicity: The single-particle wave functions $\Psi(r)$ of three-dimensional (3D)-periodic bulk, two-dimensional (2D)-periodic film/well, one-dimensional (lD)-periodic wires, or zero dimensional (0D)-periodic dot are expanded by a handful of 3D-periodic Bloch orbitals taken from the Brillouin zone center (Γ point) of the

Figure 2: Illustration of atomic processes during epitaxial nucleation process.

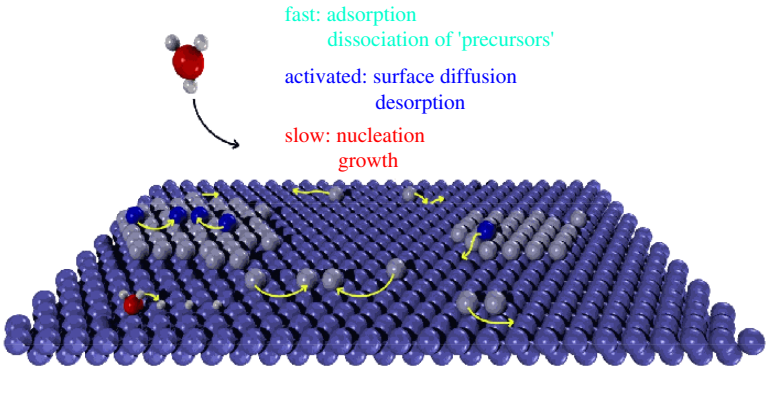

underlying bulk solid. The physical accuracy of this representation is naturally highest for systems closest to the reference from which the basis functions are drawn (Γ point of the 3D bulk). It decreases as one wanders away from the Brillouin zone center and as dimensionality (D) is reduced in the sequence 3D-to-2D-to-lD-to-0D[6]. Consequently in designing an alternative theoretical description of the electronic structure of nanostructures, the following requirements are set:

1. No adjustable parameters, except for the 3D bulk, in which "local-density approximation (LDA) errors" are corrected. The accuracy of the physical description should be the same for nanostructures of all dimensions (3D, 2D, lD, and 0D). Likewise, zone-center (Γ) and off-r states should be described equivalently. The atomistic symmetry of the object at hand should be preserved. Furthermore the distinction between the unequal symmetries of the (110) and (110) faces of InAs pyramidal dots is also lost. These misrepresentations of the true, atomistic symmetries by the continuum approach underlying the Standard Model introduced errors in the energy levels[7].
2. The real atomistic surface of the nanostructure should be included in the description rather than an (infinite) potential barrier lacking chemical personality.
3. Flexibility: The basic constructs determining the electronic structures should be incorporable in a flexible/modular manner and on equal footing. This includes the ability to incorporate different chemical species (e.g., dots made of either ionic or covalent materials), arbitrary shapes of the nanostructure, crystal-field and spin-orbit splittings, and the response to pressure and strain.

SK technique: Stranski-Kranstanow (S.K.) growth mechanism is an intermediate combination of the layer-by-layer plus island modes and ideal for QD growth.

Epitaxial Crystal Growth Modes

The many observations of Epitaxial crystal growth formation have pointed to three basic growth modes: (i) Layer by layer growth (or Frank-van der Merve), (ii) Direct island growth (or Volmer-Weber) and (iii) Layer and Island growth (or Stranski-Kranstanow), which are illustrated schematically in Fig. 3. Island growth occurs when the smallest stable clusters nucleate on the substrate and grow in three dimensions to form islands. This happens when atoms or molecules in the deposit are more strongly bound to each other than to the substrate. In layer by layer growth mode the atoms are more strongly bound to the substrate than to each other. The first complete monolayer is then covered with a somewhat less tightly bound second layer. Providing the decrease in bonding energy is continuous toward the bulk crystal value, the layer growth is sustained. The layer plus island or Stranski-Kranstanow (S.K.) growth mechanism is an intermediate combination of the aforementioned modes. In this case, after forming one or more monolayers, subsequent layer growth become unfavorable and island form[8,9].

Homo-epitaxy

Homo-epitaxy will be discussed using silicon as an example in a conventional MOCVD process. Predominantly silane (SiH_4) and chlorosilanes ($SiCl_4$, $SiHCl_3$, SiH_2Cl_2) are used as reaction gases together with a carrier gas of H_2. The process is carried out above 1000°C. The reaction gas decomposes at such temperatures to silicon, which is deposited onto the substrate surface, and gaseous Cl_2 or HCl, depending on the composition, are evolved. The reaction gas is diluted with an inert carrier gas, in order to avoid autoreaction *i.e.* to avoid a breakdown of the molecular species prior to the deposition. Furthermore, small concentrations of phosphine PH_3 or diborane B_2H_6 are added, in

Figure 3: Basic modes of Epitaxial Crystal Growth.

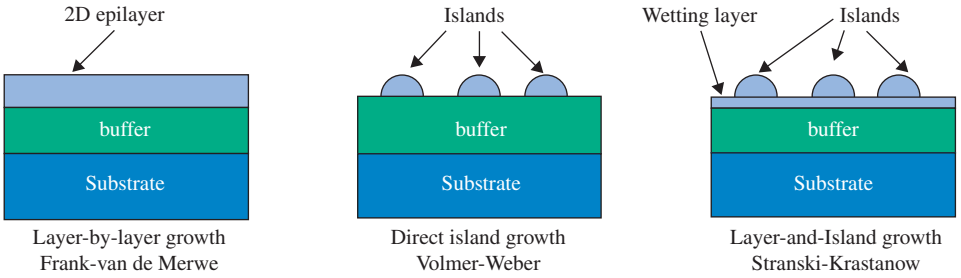

order to obtain appropriate doping of the epitaxially deposited layers. The dopant concentration is about 10^{14} to 10^{20} atoms per cm^3. Higher concentration cannot be achieved with dopants, because they would exceed the limit of solubility in silicon.

In epitaxy the deposition of the atoms take place initially on the nucleation sites on the surface. These are generally corners and edges of incomplete crystal planes. Therefore, such planes are preferentially completed by deposition, before a new crystal layer is begun. Therefore, uniform growth of a single crystal epitaxial layer is ensured. The crucial process parameters in epitaxy are temperature, concentration of the reaction gas and gas flow control, as well as crystal orientation of the host crystal. Of course the state of the substrate surface at the start of epitaxy is important. The single crystal wafer must be thoroughly cleaned of all contaminating layers, in order to propagate an undisturbed growth of the substrate. The wafer is prepared therefore, by gas phase etching which proceeds the epitaxy process. Typical growth rates for (110)-wafers are between 0.5 μm and several micrometers per minute.

Epitaxy: Epitaxy is the growth of a thin crystalline layer on a single crystalline substrate where the atoms in the growing layer mimic the arrangement of the substrate

Hetero-epitaxy

With hetero-epitaxy, crystals of different material but with the same lattice constant are built up on the host crystal. Single crystal layers of silicon on sapphire have acquired special importance. For the specific technologies special abbreviations are used:

- SOS technology: silicon on sapphire,
- ESFI technology: epitaxial silicon film on insulators,
- SOI technology: silicon on insulator

Due to high bandgap of sapphire, SOS technology allows the production of silicon

Figure 4: Evolution of the density of states as the dimensionality of the structure is reduced from 3D (bulk) to 0D (quantum dot). The density of states of an ideal quantum dot is discrete, like in an atom.

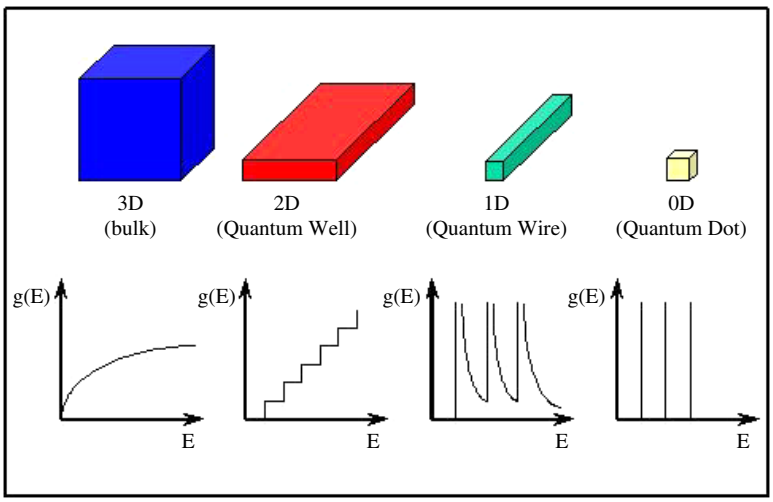

Figure 5: Schematic growth sequence with six steps for the preparation of a QD system.

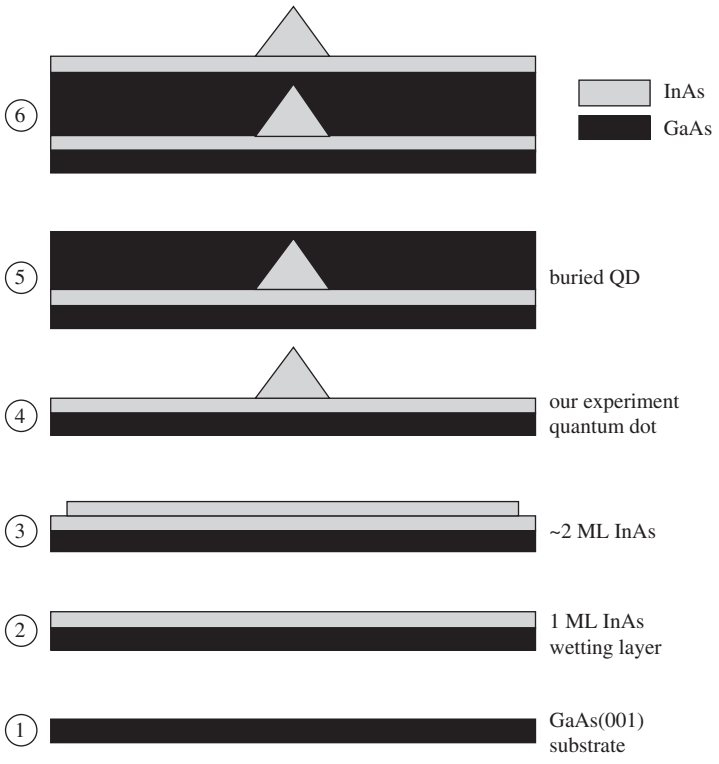

components on a sapphire chip, which even at elevated temperatures are safely insulated from each other. The deposition of epitaxial silicon layers is conducted predominantly in reactors with induction or radiation heating.

GaAs-epitaxy

Beside the silicon on sapphire technology, the deposition of GaAs on silicon is also of special technical interest. Unfortunately the lattice constants of silicon and GaAs are so different (0.5431 nm for Si and 0.5653 nm for GaAs), that these difficulties can only be overcome by very elaborate layer by layer accommodation to the different lattice constant. The current methods of epitaxy of gallium arsenide are [2]:

- CVD
- LPE (Liquid Phase Epitaxy)
- MOCVD (Metal Organic Chemical Vapor Deposition)
- MBE (Molecular Beam Epitaxy)

Binary and ternary crystal layers are frequently obtained from liquid phase epitaxy, because the stoichiometric ratio can be controlled. For GaAs generally the CVD process is used, even if the toxic reaction products in the production pose a problem.

The MBE process gives very clean, well defined epitaxial layers, in which each atomic layer can be controlled precisely. However, the rate of growth is very low (about 1 μm/h) compared with the CVD process. For these reactions the MBE process is reversed mostly for small quantities needed in research and development. A comparison is made in table 1 for accounting the features of different approaches for the epitaxy of semiconductors.

Quantum Dot Growth through Epitaxy

The first low dimensional heterostructures, known as quantum wells (QWs), were developed in early 1970s. They form the basis of most of the optoelectronic Such structures are often referred to as two dimensional (2D), because the electrical carriers (electrons and holes) are confined in a 2D plane region. The advantages of such a design are two-fold[10,11]. First, the optical properties of QWs can be tuned simply by changing their structural parameters, typically thickness and composition (so-called band-gap engineering). Secondly, the reduced dimensionality leads to improved optical performances, especially by increasing the probability of electron-hole recombination. This led scientists to investigate the possibility of reducing further the dimensionality to create 1D (quantum wire) and 0D (quantum dot) structures. For each case, there is a different density of states, as shown schematically in figure 4.

For quantum dots (QDs), the density of states becomes discrete, and for this reason, they are often described as **artificial atoms**. This property makes them interesting for fundamental studies, and quantum dots are a good candidate for the realization of quantum gates for quantum computation experiments. Also for technological applications, it was predicted[12] in 1982 that the use of QDs as the active region of a laser would provide a reduced threshold current and an improved temperature dependence. However, it has taken nearly a decade to develop reliable growth techniques that can produce quantum dots of a quality suitable for commercial applications. QD devices have now been demonstrated in many research laboratories, and commercial products are now starting to be available on the market.

Self-assembled quantum dots (QDs) have been extensively studied in recent years because of their potential for technological applications. QDs are small three dimensional ensembles of a low-band-gap semiconductor as InAs embedded in a wide-band-gap semiconductor matrix as GaAs. Such

Table 1: Comparison of epitaxial growth techniques

Techniques	Solid composition	Purity	Inherent advantages	Inherent disadvantages	Status
LPE	Thermodynamics (phase diagram)	III melt Container Gettering	Simple High purity	Volume-limited Inflexible Morphology	Laboratory technique
VPE (hydride)	Thermodynamics	Gases Leaks Reactor materials	Flexible Large scale	No AlGaAs or other Al alloys	Production technique (GaAsP)
OMVPE	Kinetics—arrival at the surface	OM sources AsH_3 C contamination Leaks	Most versatile Large scale Simple	C contamination Problems with In (?)	Potential commercial AlGaAs
MBE	Kinetics—flux sticking coefficient	Vacuum sources System (walls)	Most abrupt (2–10 Å) Low temperature	Expensive Slow r_g Problems with P	Special structures

semiconductor nanostructures exhibit quantum size effects for the localized electrons or holes: The InAs ensemble produces a confinement potential for electrons in the conduction band and for holes in the valence band. The separation between the corresponding energy levels should be larger than about 0.2 eV so that the higher lying levels are unlikely to be populated by thermal activation at room temperature. This sets an upper limit for the dot diameter of about 20 nm equivalent to about a line of 80 atoms for the diameter and about 60,000 atoms for the overall size. A lower limit is given by the condition that at least one bound level should exist which means a minimum of about 5 nm or 20 atoms in diameter and 1000 atoms in overall size. In order to achieve good intensity in electro-optical devices a number density for such QDs of about 10^{10} cm^{-2} should be reached. Furthermore, the size distribution should be rather narrow in order to produce appropriate line widths in, e.g., QD laser applications. Interestingly, laser devices operating with self-assembled InAs QDs embedded in GaAs have already been demonstrated. This development was initiated in 1990 when it was shown that dislocation-free strained InAs islands self-assemble when InAs is grown on a GaAs(0 0 1) substrate[13].

Figure 6: The schematic model of InGa and Ga droplets during As molecular beam supply for crystallization[19].

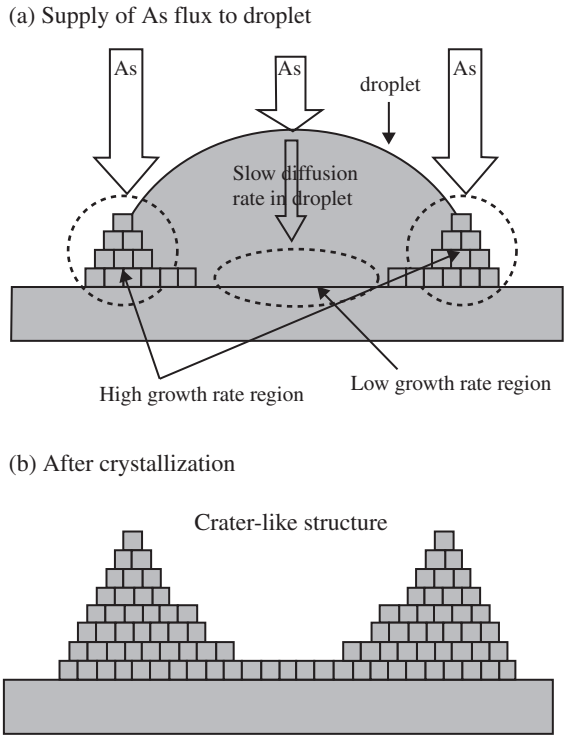

Fabrication of self-organized quantum dots (QDs) has attracted much interest from a fundamental physics and for the potential applications to optical and electronic devices such as QD lasers, single-photon source, single electron transistor and QD logic devices. Recently, **Stranski–Krastanow (S–K) growth mode** and **epitaxy droplet method** have been most commonly used for the fabrication of QDs. QDs grown by the S–K growth mode, especially InAs QD on lattice-mismatch system such as GaAs and InP, have been widely studied, because of their good optical and crystal qualities. Although there have been several reports on the droplet epitaxy to fabricate nanostructures on both lattice matched and lattice-mismatched material system, fabrication of InAs QDs via droplet epitaxy on lattice mismatched system still has some

Figure 7: Model for MBE growth of GaAs; (a) from Ga and As_2 species, (b) from Ga and As_4 species, (c) desorption of arsenic above $T_s \sim 350°C$.

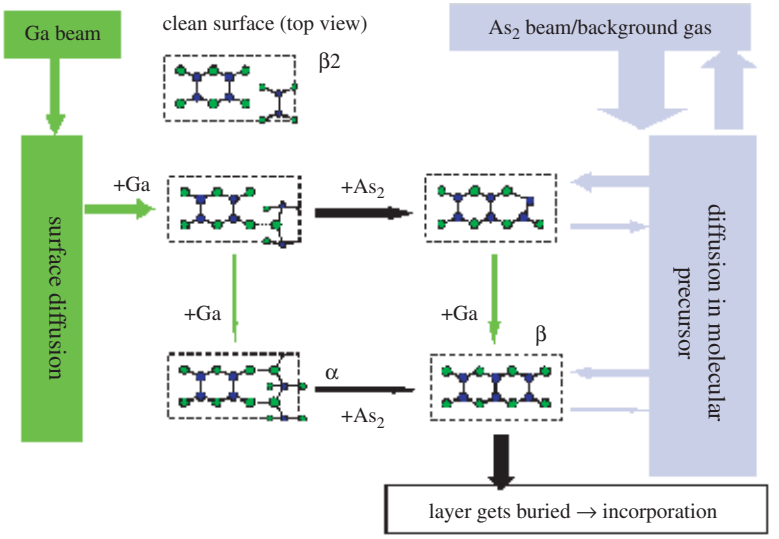

problems such as relatively low density and large size due mainly to the long migration length and high segregation effect of the newly supplied adatoms, and consequently, relatively worse optical properties compared to the conventional S–K grown QDs.

Stranski–Krastanow Growth Mode

The most common and most practical way to grow InAs/GaAs quantum dots is by using the so-called Stranski-Krastanow (SK) mode of growth. The possibility of island formation on an initially at heteroepitaxial surface was proposed in 1937 by Stranski and Krastanow and the term "SK growth" has become commonplace in the quantum dot community. It consists of depositing a material (here InAs) with a slightly larger lattice constant than the substrate (here GaAs). The small lattice mismatch (here 7%) introduces strain. During SK growth, the first few layers (here 1.6 to 2 ML of InAs) form a pseudomorphic 2D layer usually called wetting layer (WL). After this critical thickness is deposited, the two-dimensional growth is no longer favourable energetically, and the subsequent material organizes itself into 3D islands, leading to three-dimensional growth. Such islands are usually referred to as self-assembled or self-organized quantum dots. The size and density of the islands strongly depends on the growth parameters and are a result of both thermodynamic and kinetic effects. To complete the growth, the islands have to be embedded in a barrier material, usually GaAs, InGaAs, or InAlGaAs for InAs quantum dots. In recent years, the importance of this capping stage has been emphasized and it was shown that the structural properties of the dots can be modified during capping because of material redistribution and intermixing. Under the right growth conditions, the buried islands are coherent quantum dots. This means that the strain is accommodated through elastic relaxation. If the conditions are not correct, plastic relaxation can occur, for example through the formation of dislocations, in order to release the strain. Such dislocations are not desirable since they strongly reduce the luminescence efficiency[14].

The self-assemblage of QDs is understood to occur during SK growth mode in heteroepitaxy: At a critical thickness of the epitaxial InAs layer (step 3 in Fig. 5) 3-D islands or QDs form on top of a wetting layer which is largely composed of the deposited material. This process is called islanding or SK transition. These islands can be completely embedded then by additional overgrowth—-with material of the same kind as the substrate–establishing an ensemble QDs. In the SK growth mode, islands form when the strained heteroepitaxial film reaches a given thickness because the material can better relax in slightly strained islands than in a heavily strained film. Thereby the gain in elastic energy compensates for the energy cost due to the increase in surface area. The residual strain in the islands can be further reduced by incorporation of dislocations at the interface.

Droplet Epitaxy: The Ga (or In) droplets first form on the substrate surface, followed by a subsequent reaction with As to produce GaAs (or InAs) Quantum Dots. Benefits are, the Low temperature growth, and the fabrication of both lattice-matched and lattice mismatched quantum dots.

Droplet Epitaxy Method

In this method[15], the Ga (or In) droplets first form on the substrate surface. Subsequently, the droplets react with As to produce GaAs (or InAs) QDs. This method has some technology advantages such as the option of low temperature growth, and the fabrication of both lattice-matched and lattice-mismatched quantum dots. The liquid nature of the droplets also tends to produce dislocation-free and coherent nano-islands. The grown material is ideally unstrained, and sharp interfaces with reduced intermixing can be also obtained. GaAs/AlGaAs QDs cannot be created by SK growth because of the almost perfect match of lattice parameters.

Figure 6 shows the schematic model of the crystallization for InGa and Ga droplets during As molecular beam supply. The As flux is supplied to the InGa and Ga droplets formed on a Ga-stabilized surface (Fig. 6(a)). The impinging As atoms cover the entire area of surface (b). When the surface is covered with As, it is possible for In and Ga atoms to detach from the droplets and attach themselves to the nearest As atoms (c). Then, the surface will be completely covered with In or Ga (d). Processes (a)–(d) continue until the disappearance of droplets.

Figure 8: Selectively Grown InAs Nanostructures

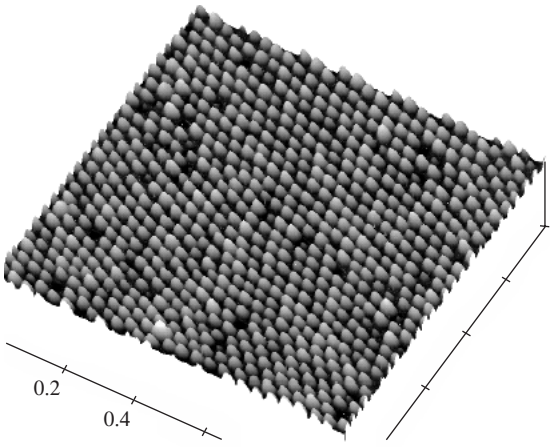

It is worth pointing out that the highly dense Ga droplets restrict the area of two-dimensional diffusion of InGa atoms from the droplets, forming the InGaAS QDs[16].

Crystallization mechanisms of GaAs nanostructures are roughly classified into two processes, as schematically illustrated in Fig. 6. The first one is GaAs growth inside the droplets by As atom diffusion into the droplets (process A). As atoms attached on the droplet surface diffuse into the droplets. When these As atoms reach the interface between the droplets and GaAs (or AlGaAs), the As and Ga atoms change into epitaxial GaAs with some probabilities. The second one is GaAs growth at the edge of the droplets (process B). Since both Ga (from the droplets) and As (from the flux) atoms are directly supplied to GaAs (or AlGaAs) surfaces, efficient crystallization is expected at this area. The two processes are correlated to each other and final shapes of the nanostructures are determined by the balance of them. Although more quantitative discussion is necessary for deeper under standing and further development, it is obvious that the shapes of the GaAs nanostructures can be simply controlled by crystallization parameters, i.e, substrate temperatures and As_4 flux intensities[17,18].

Growth of Quantum Dots by MBE

Introduction to MBE Process

Molecular beam epitaxy (MBE) is basically a sophisticated form of vacuum evaporation. Molecular beams of the constituent elements are generated from sources and travel without scattering to a substrate where they combine to form an epitaxial film. In solid source MBE, material is evaporated from solid ingots by heating. The rate of growth depends on the flux of material in the molecular beams which can be controlled by the evaporation rate and, most importantly, switched on and off with shutters in a fraction of the time required to grow one monolayer (ML). Typical growth rates are 1 ML per second, or 1 micron per hour, which is equivalent to a pressure of 10^{-6}mbar arriving at the substrate in the molecular beams. Great trouble is taken to ensure that negligible quantities of impurity atoms are introduced into the material: substrates are carefully prepared and cleaned; only ultra pure sources are used; the reaction chamber is evacuated to $< 10^{-11}$ mbar and the walls of the chamber cooled with liquid nitrogen. Even so the highest mobility layers are only grown after an extended run when the machinery has completely cleaned itself.

The basic principle of epitaxial growth is that atoms on a clean surface are free to move around

Figure 9: (a) Self assembled InAs Quantum Dots, (b) TEM cross-sectional image of InAs quantum dot on GaAs Substrate.

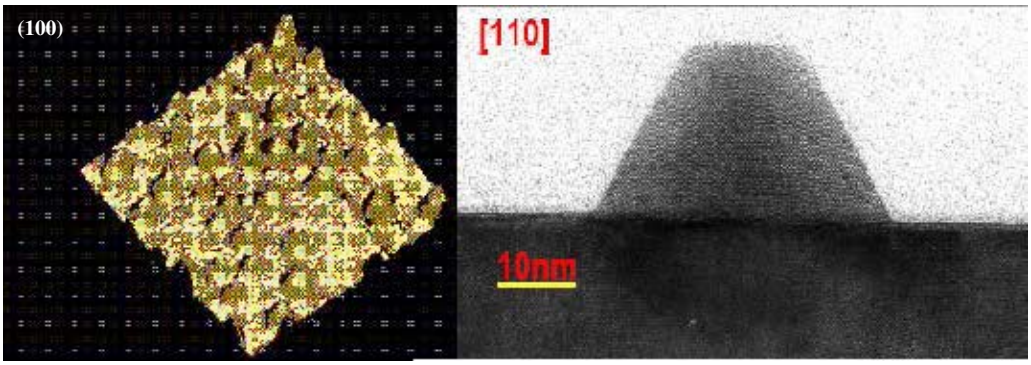

(a) (b)

Figure 10: (a) Band-diagram of InGaN QDs grown on GaN and (b) SEM picture of InGaN QDs grown on GaN.

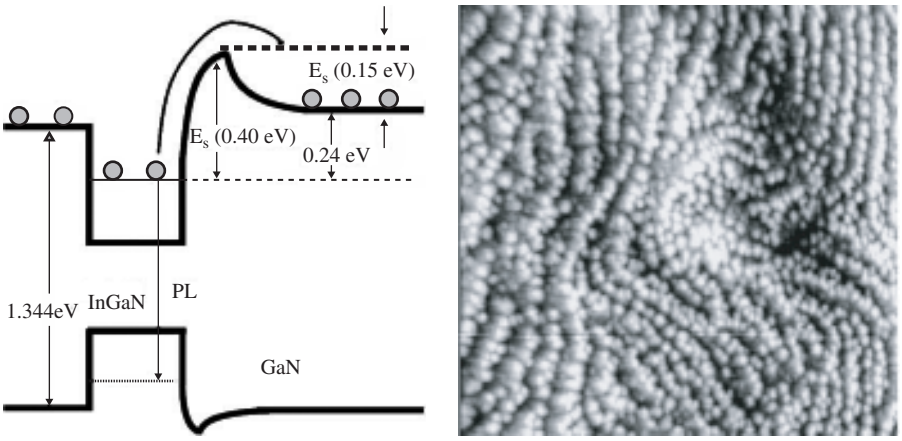

until they find a correct position in the crystal lattice to bond. Growth occurs at the step edges formed since at an edge an atom experiences more binding forces than on the free surface (see diagram). In practice there will be more than one nucleation site on a surface and so growth is by the spreading of islands. In high quality material these islands will be large with height differences of less than a ML. The mobility of an atom on the surface will be greater at higher substrate temperature resulting in smoother interfaces, but higher temperatures also lead to a lower "sticking coefficient" and more migration of atoms within the layers already grown. In practice the beams do not contain individual atoms, but molecular species like As_2 or As_4. These are *cracked* at the surface and the efficiency of the process is also temperature dependent. Clearly there will be a compromise temperature to achieve the best results. For GaAs this is ~600° C.

The surface chemical processes involved in the MBE growth of binary and ternary III-V compounds were studied extensively using a combination of modulated molecular beam techniques and reflection high energy electron diffraction (RHEED). From these results, rather detailed kinetic models are now available for the growth of GaAs from beams of Ga and As_2 and Ga and As_4 (Figure 7). Ga has a unity sticking coefficient on (100) GaAs at 480°C. Above this temperature Ga is adsorbed as well as desorbed[20].

Variations in Quantum Dot Formations

Semiconductor quantum dots (QD's) are expected to dramatically improve the performance of optoelectronic devices due to 3-D quantum confinement[21]. So far, two methods are mainly used for fabricating QD structures. One method utilizes the complicated lithography, etching, and then regrowth processes. Due to the limitation imposed by the current lithographic techniques, the QD's fabricated by this method usually have larger sizes and lower densities than the desirable values (Figure 8). Furthermore, the QD's can be contaminated during the etching process and they may have high defect densities.

Another method utilizes a phase transition from a deposited layer of a few monolayers thick on a buffer layer to 2-D islands due to lattice mismatch between the two epitaxial layers. For example, InAs QD's can be readily formed on the top of a GaAs buffer layer. Such a type of the QD's can be incorporated into many optoelectronic devices with greatly-improved performances. A laser diode based on the QD's exhibits a much lower threshold. This simple method has an advantage of reaching small sizes and high densities. However, as a result of self-assembling process the size of the QD's usually fluctuates within ±10%. Recently, strain-induced quantum-well (QW) nanostructures, i.e. self-assembled quantum dots grown on the top of a single quantum well (QD's:QW or QWD's), have attracted much attention, since such structures can be in principle defect-free. So far, most of the QD's and QWs are based on the InGaAs and InGaP QW's strained by the InP QD's. Since the QW thickness can be controlled within a subatomic layer, the size fluctuation of the strain-induced QD's is expected to be substantially reduced. Moreover, the interface and surface recombination rates can be significantly reduced. Furthermore, since the QD's and QWs are

Figure 11: (a) STM image of InAs QDs on GaAs(0 0 1). InAs was deposited at 450°C at a rate of 0.05 Å sec^{-1} (sample bias voltage U = −2.25 V; sample current I = 0.19 nA). The number density of the QDs is $1.9 \times 10^{11} cm^{-2}$. (b) Histogram of QD sizefrom the STM image in (a).

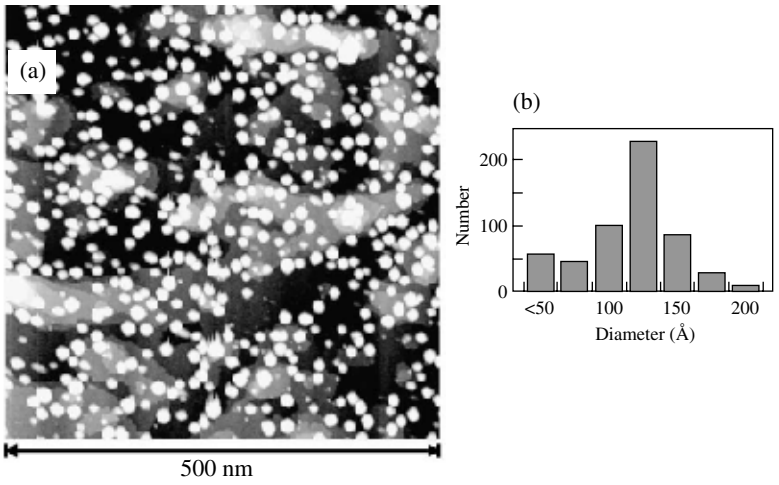

formed inside the QW layer, the capture rate for photogenerated carriers can also be improved[22].

RHEED: Reflection High Energy Electron Diffraction monitors the growth pattern at each monolayer formation level and growth strains residing during growth.

The formation of three-dimensional InAs islands on a GaAs surface is a complex interplay of local strain and adatom migration length (which depends on the flux and substrate temperature) (Figure 9). Using probe microscopy (STM and AFM) one can demonstrate that the island composition depends strongly on the temperature and indium flux. For long wavelength applications the composition should be close to pure InAs. This can be achieved by depositing the InAs at a low rate, typically a factor of 20 less than that used by other groups. In order to access even longer wavelengths the strain state of the dot must be controlled. This can be achieved through the use of seed layers that provide a template for second and subsequent layers of dots. Careful control of the spacer thickness and capping procedure inhibit segregation effects.

Few Examples of Materials for Quantum Dots

GaN-InGaN

Group III nitride-based structures have great attraction due to their large band-gap energies for optoelectronic devices[23,24]. InGaN/GaN heterostructures form the active layer in blue-green LEDs and laser diodes commercially available today. The performance of quantum dot (QD) structures could still be improved enormously, because QDs are expected to provide carrier localization centers with negligible compositional fluctuation. In particular, InGaN QD lasers are expected to have low threshold current densities and good temperature stability compared with conventional blue lasers with InGaN quantum wells. In order to study the properties of InGaN QDs, most research groups have used optical methods such as photoluminescence (PL). Of course, such methods provide very important information to apply a QD structure to optical and electrical devices.

It has been demonstrated that an interrupted growth mode can be used to fabricate nanoscale InGaN self-assembled QDs using MBE technique (Figure 10). InGaN QDs successfully form with a lateral size of 25nm and a height of about 4.1nm during interrupted growth of QDs by MOCVD. The interrupt time employed was 12 seconds and the QD density was of $2 \times 10^{10} cm^{-2}$. In a typical growth process, the interrupted growth mode method was employed as follows. First 4.5MLs of InGaN were deposited on top of a GaN buffer layer; then, the growth was stopped for a time period of 12 seconds. After the growth stop, another 4.5MLs of InGaN were again deposited so as to achieve an InGaN layer with a total thickness of about 9.0MLs. Without using the interrupted growth mode method, with same growth conditions, another sample was prepared by directly depositing 9MLs of InGaN for comparison, as can be seen in figure 10(b) through AFM characterization.

InAs/GaAs QDs Grown by S-K mode

We now turn to measurements of InAs QDs on GaAs(0 0 1)[25,26] Fig. 11(a) gives an overview STM on a 500×500 nm^2 scale. From visual inspection of Fig. 11(a) as well as from the diagram in Fig. 11(b) one recognizes that the size distribution of the QDs is relatively sharp. Fig. 11(a) contains 489 QDs

Figure 12: InAs/GaAs self-assembled quantum dot.

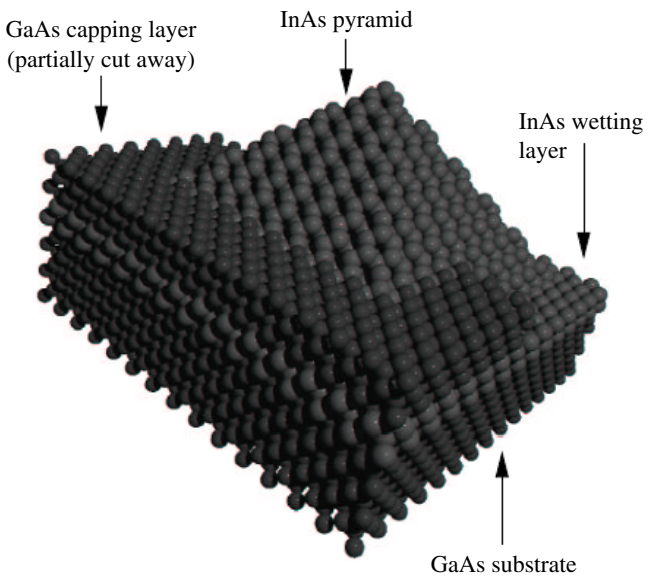

which is equivalent to a number density of 1.9×10^{11} QDs cm^{-2}. About half of the QDs have a diameter of 12.5 ± 1.0 nm and the mean height is 2.2 nm resulting in an aspect ratio of AR = 0.18. Large-area changes in brightness in the background of Fig. 11 are due to the structure of the wetting layer and especially due to mono-atomic steps [5]. A typical atomic arrangement during the growth of quantum dots, is shown for illustration inn figure 12.

QDIP: Quantum-dot Infra-red photodetectors are intrinsically photovoltaic, and originates primarily from the geometric shape of the dots. The physical structure of the dot has no plane of symmetry perpendicular to the growth direction.

The growth of lattice-mismatched heteroepitaxial structures follows mechanisms that are different from those described for the 2D MBE growth[27,28]. With reference to the growth on GaAs of the 7% lattice-mismatched InAs (Fig. 13), during the initial stage of deposition, InAs grows following the layer-by-layer 2D mechanism with the in-plane lattice parameter matched to that of the underlying GaAs substrate; the resulting strained layer is termed as a wetting layer (WL). The corresponding RHEED pattern shows the arrangement of streaks typical of the InAs (100) reconstruction (Fig. 13c). When the amount of deposited InAs exceeds the so called critical coverage (θ_c), the streaks are suddenly replaced by bright spots (Fig. 13e), thus indicating that the 2D layer-by-layer growth mode is no longer followed and that the growth proceeds by the formation of 3D islands (Fig. 13f). θ_c depends both on the growth conditions and on the lattice mismatch of the heterostructure: a typical value for InAs deposited on (001) GaAs is $\theta_c = 1.6$ ML ($\sim$0.5 nm). The well-known evolution described in Fig. 13e, f is usually referred as 2D-to-3D growth transition ; the nucleation of 3D islands homogeneously distributed on the growing surface. The islands are nanometre-sized, with heights and diameters in the order of few nanometres and few tens of nanometres, respectivelyThe growth of self-assembled 3D islands on top of a 2D wetting layer pseudomorphically grown on the underlying epilayer, is usually referred to as Stranski-Krastanow 3D growth.

Few examples of Device Applications:

Several devices are under active development across the community of semiconductors. Few examples are chosen for the present discussion, as they are also actively pursued at Materials Research Centre, Indian Institute of Science, Bangalore.

QDIPs (Quantum Dot Infrared Photodetectors

There are two possible kinds of device structures for a quantum-dot infrared photodetector[29,30]; this classification is based on the direction in which the photocarriers move[31]. The conventional photodetector structure is shown in the figure. The photoelectrons in this structure move along the (perpendicular) growth direction when a static electric field is applied normal to the plane of the quantum-dot layers[32]. The typical quantum-dot photodetector (Figure 14) consists of, from the substrate up, a heavily doped n-type, 1.0μm-GaAs bottom contact layer, followed by an infrared-sensitive active region composed of either a quantum-dot superlattice structure or a single quantum-dot layer; the active region is terminated by a top, heavily doped, n-type GaAs cap layer. The device is essentially a fancy, photosensitive resistor. The GaAs barrier layers in the structures typically range from about 30 to 50 nm; these are sufficiently thick that the vertical quantum-mechanical coupling between the dots can be ignored. The InGaAs quantum-dot layers are doped with silicon. Quantum-dot photodetectors are intrinsically photovoltaic. This property originates primarily from the geometric shape of the dots. The physical structure of the dot has no plane of symmetry perpendicular to the growth direction. This asymmetry in structure can, and does, lead to experimentally observable effects. The measured photovoltaic responsivity is about 1 mA/W (at zero bias voltage). The responsivity is zero at the bias voltage of 0.36 V. This voltage is dropped across the 20-period quantum-dot superlattice. The potential drop across each layer is therefore about 18 mV; this voltage is generally referred to as the compensation voltage. As already discussed above, a photovoltaic effect, such as the one observed here, usually indicates the presence of a built-in

Figure 13: RHEED patterns (panels a, c and e) during the 2D deposition of GaAs (b), the 2D deposition of InAs (d) and the 3D deposition of InAs (f) on a (100) GaAs buffer layer, respectively.

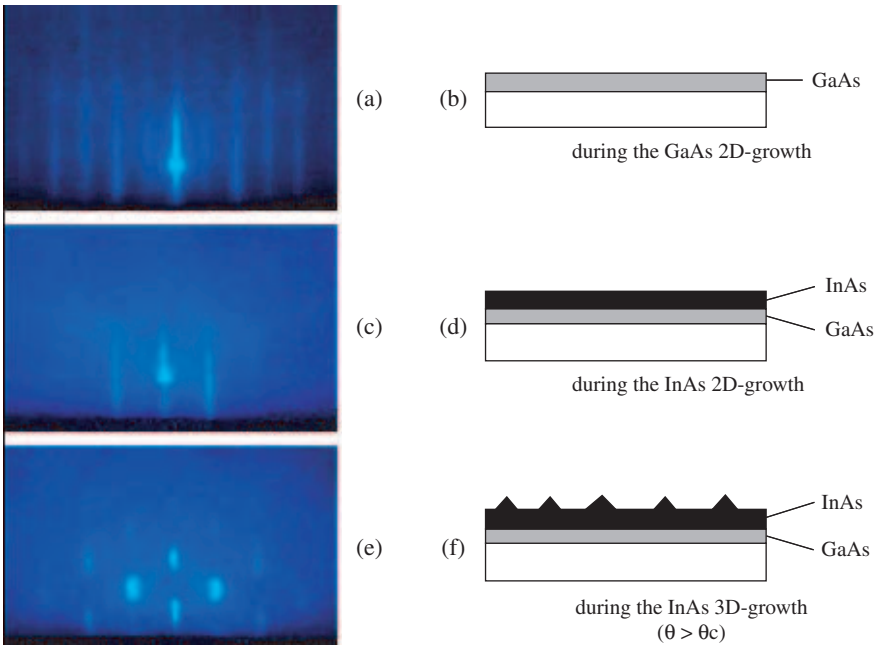

Single Photon source: Single Quantum Dots obtained by strain-driven nucleation in the Stranski–Krastanov growth mode emit single photons.

electrical field. Because self-organized quantum dots are intrinsically asymmetric with respect to the growth plane, the inherent strain distribution, and the band structure of the quantum dots will also be asymmetric. Because the wetting layers in the structures introduce a shallower potential than do the dots, an overall asymmetrical band structure is naturally formed. In addition to the asymmetric effect of the wetting layer, the dots are also asymmetric with respect to the growth plane because of their shape which can be pyramidal or plano-convex lens-shaped, depending on the growth conditions. The shape of the dots, therefore, further increases the degree of asymmetry of the band structure of the detector layers. Electrons in the excited state of such a structure are swept across by the built-in field, thus contributing to the photocurrent. Because quantum dots' electron energy levels are discrete rather than continuous, the addition or subtraction of just a few atoms to the quantum dot has the effect of altering the boundaries of the bandgap. Changing the geometry of the surface of the quantum dot also changes the bandgap energy, owing again to the small size of the dot, and the effects of quantum confinement. The bandgap in a quantum dot will always be energetically larger; therefore, we refer to the radiation from quantum dots to be "blue shifted" reflecting the fact that electrons must fall a greater distance in terms of energy and thus produce radiation of a shorter, and therefore "bluer" wavelength. As with bulk semiconductor material, electrons tend to make transitions near the edges of the bandgap. However, with quantum dots, the size of the bandgap is controlled simply by adjusting the size of the dot. Because the emission frequency of a dot is dependent on the bandgap, it is therefore possible to control the output wavelength of a dot with extreme precision.

Single Photon Source

Conventional sources of light, such as light-emitting diodes and lasers, generate radiation that can be successfully described with classical Maxwell's equations. On the other hand, several applications in the emerging field of quantum information science require weak optical sources with strong quantum correlations between single[33]. This is particularly true for quantum cryptography, which exploits the fundamental principles of quantum mechanics to provide unconditional security for communication. An essential element of secure key distribution in quantum cryptography is an optical source emitting a train of pulses that contain one and only one photon[34].

Because measurements unavoidably modify the state of a single quantum system, an eavesdropper cannot gather information about the secret key

Figure 14: Schematic diagram showing the heterostructure of a typical QDIP.

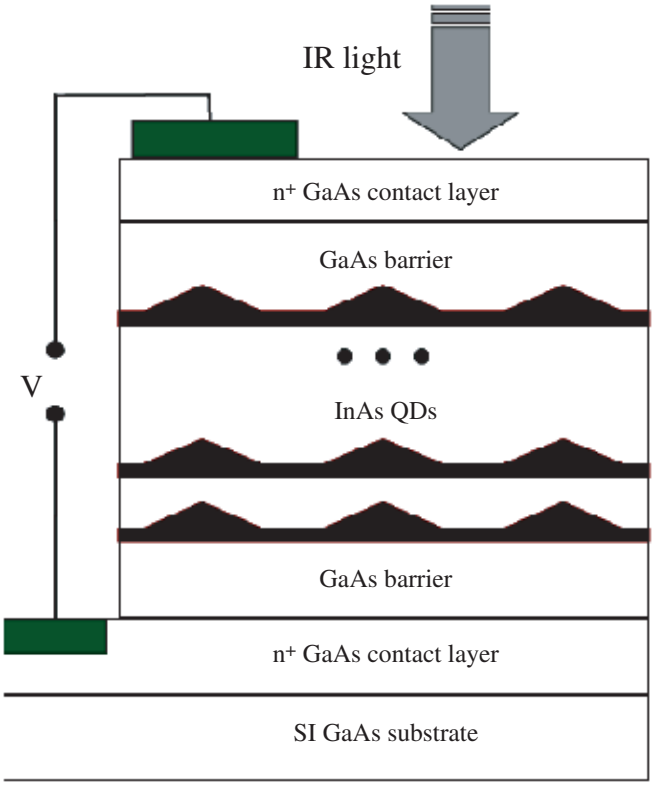

without being noticed, provided that the pulses used in transmission do not contain two or more photons. More recently, it has also been shown that the availability of a single-photon source enables implementation of quantum computation using only linear optical elements and photodetectors (Figure 15). A single photon source uses the anharmonicity of single quantum dot (QD) multi-exciton transitions to regulate the photon generation process. Realization of such a source, termed a single-photon turnstile device, has been one of the holy grails of quantum electronics research, because it represents the ultimate limit in the quantum control of the photon generation process.

Figure 15: Schematic of InAs (QDs) /GaAs based single photon source[35].

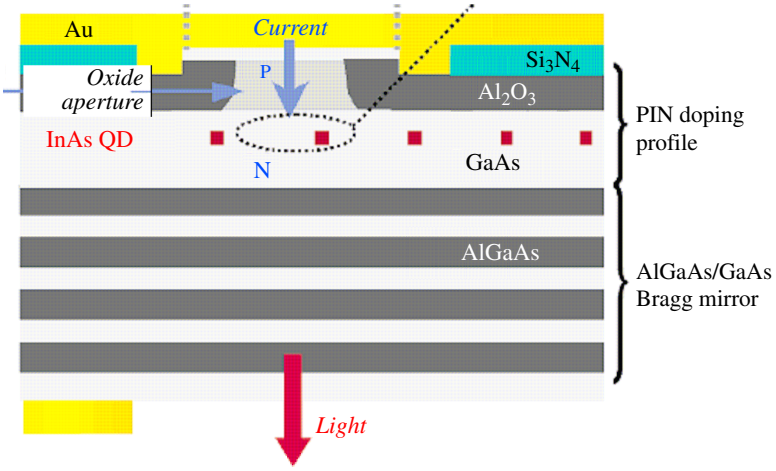

It is known that a driven single anharmonic quantum system, such as an atom or a molecule, exhibits photon anti-bunching; that is, a dead time between successive photon emission events. With the use of Hanbury-Brown and Twiss (HBT)-type photon correlation measurements, photon anti-bunching has been observed in a variety of single quantum emitters, for example, an atom, a stored ion, a molecule, and a semiconductor QD. Photon anti-bunching is a necessary but not sufficient condition for a single-photon turnstile device; an additional mechanism for regulating the excitation process is required to realize single-photon pulses. A single-photon turnstile device based on a mesoscopic double-barrier p-n heterojunction was proposed in 1994. This device uses Coulomb blockade of tunneling for electrons and holes in a mesoscopic p-n diode structure to regulate the photon generation process. In this scheme, single-electron and hole-charging energies must be large compared to the thermal background energy to ensure single-photon emission. Therefore, this device can only be operated at ultra-low temperatures ($T \leq 1$ K). With the use of photon correlation measurements, it was concluded that approximately 74% of the pulses give rise to single-photon emission at 1.8 K, with a repetition rate of a few megahertz. The single-photon source is based on a single QD embedded in a high-quality factor (Q) micro-cavity structure. The distinguishing feature of the QD single-photon source is the absence of pulses that contain more than one photon. To ensure single-photon generation at the fundamental QD exciton transition (1X), the pump power is adjusted so that two or more electron-hole pairs are captured by the QD during each excitation pulse. The energy of the photons emitted during relaxation depends significantly on the number of multi-excitons that exist in the QD, due to Coulomb interactions enhanced by strong carrier confinement. If the total recombination time of the multi-exciton QD state is longer than the recombination time of the free electron-hole pairs, each excitation pulse can lead to at most one photon emission event at the 1X transition. Therefore, regulation of the photon emission process can be achieved because of a combination of Coulomb interactions

creating an anharmonic multi-exciton spectrum and slow relaxation of highly excited QDs leading to a vanishing re-excitation probability after the photon emission event at the 1X transition. If the QD exciton recombination is predominantly radiative, every excitation pulse from the mode-locked laser will generate an ideal single-photon pulse. When the QD 1X transition is on resonance with a high-Q cavity mode, the spontaneous emission rate is enhanced because of the Purcell effect. In addition to reducing the time jitter in photon emission and thereby allowing for a higher single-photon pulse repetition rate, the Purcell effect could also ensure that radiative recombination dominates over nonradiative relaxation mechanisms.

Received 02 February 2007; revised 26 March 2007.

References

1. D. Loss and D. DiVincenzo, *Quantum computation with quantum dots*, Phys. Rev. A 57, 120–126 (1998).
2. J. M. Elzerman, R. Hanson, L. H. Willems Van Bereven, B. Witkamp, L. M. Vandersypen, and L. P. Kouwenhoven, *Single-shot read-out of an individual electron spin in a quantum dot*, Nature 430, 431 (2004).
3. G **B** Stringfellow, Rep. Prog. Phys., Vol. 45, 1982. Printed in Great Britain.
4. Bruce A. Joycea, Tim B. Joyce, Journal of Crystal Growth 264 (2004) 605–619.
5. A. G. U. Perera and H. C. Liu (eds), *Semiconductor Optical and Electro- Optical Devices, Handbook of Thin Film Devices 2*, Academic Press, 2000
6. A. Rogalski, *Progress in Quantum Electronics* **27**, 59 (2003)
7. H. C. Liu and F. Capasso (eds), *Intersubband Transitions in Quantum wells: Physics and Device Applications I, Semiconductor and Semimetals* **62**, Academic Press, 2000
8. Rep. Prog. Phys., Vol. 45, 1982. Printed in Great Britain
9. Ploog K 1980 *Crystal Growth, Properties, Applications* ed H ***C*** Freyhardt (Berlin: Springer-Verlag) pp 75
10. T. Mano, N. Koguchi, Journal of Crystal Growth 278 (2005) 108–112.
11. S. Franchi, G. Trevisi, L. Seravalli, P. Frigeri, Progress in Crystal Growth and Characterization of Materials 47 (2003) 166–195.
12. Y. Arakawa and H. Sakaki, Appl. Phys. Lett. **40**, 939 (1982).
13. K. Jacobi, Progress in Surface Science 71 (2003) 185–215.
14. E. C. Le Ru, P. Howe, T. S. Jones, and R. Murray, Phys. Rev. B **67**, 165303 (2003).
15. T. Mano, K. Watanabe, S. Tsukamoto, H. Fujioka, M. Oshima and N. Koguchi, Japanese Journal of Applied Physics, 38, 603-608, L1009–L1011 (1999)
16. T. Mano, K. Watanabe, S. Tsukamoto, Y. Imanaka, T. Takamasu, H. Fujioka, G. Kido, M. Oshima and N. Koguchi, Japanese Journal of Applied Physics, 39, 4580–4583 (2000)
17. K. Watanabe, N. Koguchi, K. Ishige, C. D. Lee, J. Y. Leem, H. J. Lee and S. K. Noh, Journal of the Korean Physical Society, 38(1), 25–28 (2001)
18. N. Koguchi, Journal of the Korean Physical Society **45**, 650–655 (2005)
19. T. Mano, K. Watanabe, S. Tsukamoto, H. Fujioka, M. Oshima & N. Koguchi, J. Cryst. Growth, 209, 504–508, (2000)
20. Atomistic DFT Studies to macroscopic properties, P. Kratzer, Fritz-Haber-Institut der MPG, Germany, p23–54, (2003)
21. L. Wang, A. Rastelli, S. Kiravittaya, R. Songmuang, O. G. Schmidt, B. Krause, & T. H. Metzger, Nanoscale Res Lett (2006) 1:74–78
22. M. Henini, Nanoscale Res Lett (2006) 1:32–45
23. G. N. Panin,a! Y. S. Park, and T. W. Kang, T. W. Kim, K. L. Wang and M. Bao, Journal Of Applied Physics **97**, 043527, (2005)
24. Jeong-Sik Lee, Satoru Tanaka, Peter Ramvall, and Hiroaki Okagawa, Mat. Res. Soc. Symp. Proc. Vol. 798, (2004)
25. J. Tatebayashi, M. Nishioka, and Y. Arakawa, Appl. Phys. Lett. **78**, 3469 (2001).
26. C. Le Ru, P. Howe, T. S. Jones, & R. Murray, Phys. Rev. B **67**, 165303 (2003).
27. Cusack, M. A. PhD Thesis, .Electronic and Optical Properties of Semiconductor Quantum Wells and Dots., University of Newcastle upon Tyne. (1999).
28. S. Birudavolu, N. Nuntawong, G. Balakrishnan, Y. C. Xin, S. Huang, S. C. Lee, S. R. J. Brueck, C. P. Hains, and D. L. Huffakera, Applied Physics Letters Volume 85, Number 12 20 (2004)
29. H.C. Liu, Opto-Electronics Review **11**(1), 1–5 (2003)
30. Antoni Rogalski, Progress in Quantum Electronics 27 , 59–210, (2003)
31. D. Pal and E. Towe, Journal Of Applied Physics **100**, 084322, (2006)
32. H. D. Nam1, 2, J. D. Song1, W. J. Choi1*, J. I. Lee1, H. S. Yang, Mater. Res. Soc. Symp. Proc. Vol. 864, (2005)
33. B. Alloing, C. Zinoni, V. Zwiller, L. H. Li, C. Monat, M. Gobet, G. Buchs, and A. Fiore, Applied Physics Letters **86**, 101908 (2005)
34. Irene D'Amico & Fausto Fossi, Applied Physics Letters Volume 81, 27, (2002)
35. Christelle Monat,* Blandine Alloing, Carl Zinoni, Lianhe H. Li, And Andrea Fiore, Nano Letters, Vol. 6, No. 7, 1464–1467, (2006)

Dr. S.B. Krupanidhi is a Professor at Materials Research Centre, Indian Institute of Science, Bangalore. Prior to that, he served at Pennsylvania state university, USA; Motorola, Albuquerque, USA; and Queens University, Canada at various levels of scientific designations. He integrates in an exemplary manner fundamental science with engineering of materials and devices. He is internationally recognized in the areas of integrated ferroelectrics and compound semiconductor technology. Professor Krupanidhi's research is focused on developing epitaxial thin films of complex oxides for electro-optic, ferroelectric, and high permittivity dielectric applications and hetero epitaxial compound semiconductors for opto-electronic applications. Primary focus is to develop low temperature epitaxy compatible with the existing semiconductor technology. During the last decade, his primary mission was to develop radiation hard non-volatile memories and dynamic random access memories (DRAMs), piezoelectric micro-actuators and motors (MEMS), Quantum wells and quantum dots of III–V compound semiconductors. He has authored more than 300 research papers in international journals and also authored chapters in various books.